Electrostatically-tuned superconductor-metal-insulator quantum transition at the $LaAlO_3/SrTiO_3$ interface

T. Schneider,[1,*] A. D. Caviglia,[2] S. Gariglio,[2] N. Reyren,[2] and J.-M. Triscone[2]
[1]*Physik-Institut der Universität Zürich, Winterthurerstrasse 190, CH-8057 Zürich, Switzerland*
[2]*DPMC, University of Geneva, 24 Quai Ernest-Ansermet, 1211 Geneva 4, Switzerland*
(Received 8 February 2009; revised manuscript received 26 March 2009; published 1 May 2009)

Recently superconductivity at the interface between the insulators $LaAlO_3$ and $SrTiO_3$ has been tuned with the electric-field effect to an unprecedented range of transition temperatures. Here we perform a detailed finite-size scaling analysis to explore the compatibility of the phase-transition line with Berezinskii-Kosterlitz-Thouless (BKT) behavior and a two-dimensional–quantum-phase (2D-QP) transition. In an intermediate regime, limited by a gate voltage dependent limiting length, we uncover remarkable consistency with a BKT-critical line ending at a metallic quantum critical point, separating a weakly localized insulator from the superconducting phase. Our estimates for the critical exponents of the 2D-QP-transition, $z \simeq 1$ and $\bar{\nu} \simeq 2/3$, suggest that it belongs to the three-dimensional-xy universality class.

DOI: 10.1103/PhysRevB.79.184502 PACS number(s): 74.40.+k, 74.90.+n, 74.78.Fk

I. INTRODUCTION

At the interface between oxides, electronic properties have been generated, different from those of the constituent materials.[1–3] In particular, the interface between $LaAlO_3$ and $SrTiO_3$, two excellent band insulators, found to be conducting in 2004 (Ref. 1) attracted a lot of attention.[4–9] Recently, different ground states, superconducting and ferromagnetic, have been reported for this fascinating system.[2] In a recent report,[10] it was shown that the electric-field effect can be used to map the phase diagram of this interface system revealing, depending on the doping level, a superconducting and nonsuperconducting ground state and evidence for a quantum-phase transition.

Continuous quantum-phase transitions are transitions at absolute zero in which the ground state of a system is changed by varying a parameter of the Hamiltonian.[11–13] The transitions between superconducting and insulating behavior in two-dimensional systems tuned by disorder, film thickness, magnetic field or with the electrostatic field effect are believed to be such transitions.[12–19]

Here we present a detailed finite-size scaling analysis of the temperature and gate voltage dependent resistivity data of Caviglia *et al.*[10] to explore in the $LaAlO_3/SrTiO_3$ system the nature of the phase-transition line and of its end point, separating the superconducting from the insulating ground state. For this purpose we explore the compatibility of the normal state to superconductor transition with Berezinskii-Kosterlitz-Thouless (BKT) critical behavior.[20,21] Our analysis of the temperature dependence of the sheet resistance at various fixed gate voltages uncovers a rounded BKT transition. The rounding turns out to be fully consistent with a standard finite-size effect whereupon the correlation length is prevented to grow beyond a limiting length L. Indeed, a finite extent of the homogeneous domains will prevent the correlation or localization length to grow beyond a limiting length L and, as a result, a finite-size effect occurs. Because the correlation length does not exhibit the usual and relatively slow algebraic divergence as T_c is approached, the BKT-transition is particularly susceptible to such finite-size effects. Nevertheless, for sufficiently large L the critical regime can be attained and a finite-size scaling analysis provides good approximations for the limit of fundamental interest, $L \to \infty$.[12,22,23]

As will be shown below, our finite-size scaling analysis uncovers close to the QP transition a gate voltage dependent limiting length. According to this electrostatic tuning does not change the carrier density only but the inhomogeneity landscape as well. The finite-size scaling analysis also allows us to determine the gate voltage dependence of the BKT-transition temperature T_c, of the associated fictitious infinite system. This critical line, T_c versus gate voltage, ends at a quantum critical point at the gate voltage V_{gc}. Here the sheet conductivity tends to $\sigma_\square(T=0, V_{gc}) \simeq 2.52 \times 10^{-4}(\Omega^{-1})$ which is comparable to the quantum unit of conductivity $4e^2/h \simeq 1.55 \times 10^{-4}(\Omega^{-1})$ for electron pairs, emphasizing the importance of quantum effects. Its limiting T^2 temperature dependence points to Fermi-liquid behavior at quantum criticality. The estimates for the critical exponents of the two-dimensional–quantum-phase (2D-QP) transition, $z \simeq 1$ and $\bar{\nu} \simeq 2/3$, suggest that it belongs to the three-dimensional (3D)-xy universality class. In the normal state we observe non-Drude behavior, consistent with the evidence for weak localization. To identify the nature of the insulating phase from the temperature dependence of the resistance, we perform a finite-size scaling analysis, revealing that the growth of the diverging length associated with weak localization is limited and gate voltage dependent as well. Nevertheless, we observe in both, the temperature and magnetic-field dependence of the resistance, the characteristic weak localization behavior, pointing to a renormalized Fermi liquid. In addition we explore the T_c dependence of the vortex core radius and the vortex energy. These properties appear to be basic ingredients to understand the variation of T_c. In the superconducting phase we observe consistency with the standard quantum scaling form for the resistance, while in the weakly localized phase it appears to fail. In contrast to the quantum scaling approach we obtain the scaling function in the superconducting phase explicitly. It is controlled by the BKT-phase transition line and the vortex energy.

In Sec. II we sketch the theoretical background and present the detailed analysis of the resistivity data of Caviglia *et al.*[10] We close with a brief summary and some discussion.

II. THEORETICAL BACKGROUND AND DATA ANALYSIS

A. BKT transition

To explore the compatibility with BKT critical behavior we invoke the characteristic temperature dependence of the correlation length above T_c,[21]

$$\xi(T) = \xi_0 \exp[2\pi/(bt^{1/2})], \quad t = |T/T_c - 1|, \tag{1}$$

where ξ_0 is the classical vortex core radius and b is related to the energy needed to create a vortex.[24–27] Note that b also enters the temperature dependence of the magnetic penetration depth λ below the universal Nelson-Kosterlitz jump,[24]

$$\lambda^2(T_c)/\lambda^2(T) = (1 + b|t|^{1/2}/4). \tag{2}$$

Moreover, b is related to the vortex energy E_c in terms of[26,28]

$$b = f[E_c/(k_B T_c)]. \tag{3}$$

Invoking dynamic scaling the resistance R scales in $D=2$ as[12]

$$R \propto \xi^{-z_{cl}}, \tag{4}$$

where z_{cl} is the dynamic critical exponent of the classical dynamics. z_{cl} is usually not questioned to be anything but the value that describes simple diffusion: $z_{cl}=2$.[29] Combining these scaling forms we obtain

$$\frac{R(T)}{R_0} = \left[\frac{\xi_0}{\xi(T)}\right]^2 = \exp[-b_R(T - T_c)^{-1/2}], \tag{5}$$

with

$$b_R = 4\pi T_c^{1/2}/b, \quad R_0 \propto 1/\xi_0^2. \tag{6}$$

Accordingly the compatibility of experimental resistivity data with the characteristic BKT behavior can be explored in terms of

$$(d \ln R/dT)^{-2/3} = (2/b_R)^{2/3}(T - T_c). \tag{7}$$

Because the correlation length does not exhibit the usual and relatively slow algebraic divergence as T_c is approached [Eq. (1)] the BKT transition is particularly susceptible to the finite-size effect. It prevents the correlation length to grow beyond a limiting lateral length L and leads to a rounded BKT transition. Nevertheless, for sufficiently large L the critical regime can be attained and a finite-size scaling analysis allows good approximations to be obtained for the limit $L \to \infty$ (Refs. 12 and 22) including estimates for T_c, b_R, R_0, and their gate voltage dependence. In the present case potential candidates for a limiting length include the finite extent of the homogenous regions and the failure to cool the electron gas down to the lowest temperatures. In the latter case L is given by the value of the correlation length at the temperature where the failure of cooling sets in. In any case finite-size scaling predicts that $R(T,L)$ adopts the form

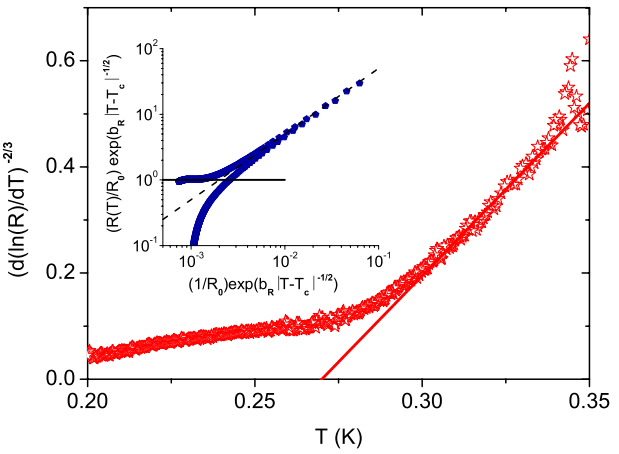

FIG. 1. (Color online) $(d \ln R/dT)^{-2/3}$ vs T for $V_g=40$ V where $R=3/5R_\square$. The solid line is $(d \ln R/dT)^{-2/3}=6.5(T-T_c)$ yielding the estimates $T_c=0.27$ K and $(2/b_R)^{2/3}=6.5$; the inset shows $R(T)\exp(b_R|T-T_c|^{-1/2})/R_0$ vs $(1/R_0)\exp(b_R|T-T_c|^{-1/2})$ with $R_0=1.67$ kΩ. The upper branch corresponds to $T>T_c$ and the lower one to $T<T_c$. The solid line is $R(T,L) \simeq R(T,\infty)$ and the dashed one $R\exp(b_R|T-T_c|^{-1/2})/R_0=(g/R_0)\exp(b_R|T-T_c|^{-1/2})$ with $g \simeq 501 \propto 1/L^2$.

$$\frac{R(T,L)}{R(T,\infty)} = \left(\frac{\xi(T,0)}{\xi(T,\infty)}\right)^2 = g(x) = \frac{R(T,L)}{R_0}\exp(b_R|T - T_c|^{-1/2}), \tag{8}$$

where

$$x = \frac{\exp(b_R|T - T_c|^{-1/2})}{R_0 L^2} \propto \left(\frac{\xi(T,\infty)}{L}\right)^2. \tag{9}$$

$g(x)$ is the finite-size scaling function. If $\xi(T,\infty)<L$ critical behavior can be observed as long as $g(x) \simeq 1$, while for $\xi(T,\infty)>L$ the scaling function approaches $g(x) \propto x$ so $R(T)\exp(b_R|T-T_c|^{-1/2})/R_0$ tends to $(g/R_0)\exp(b_R|T-T_c|^{-1/2})$ with $g \simeq 1/L^2$.

We are now prepared to explore the evidence for BKT behavior. In Fig. 1 we show $(d \ln R/dT)^{-2/3}$ vs T for $V_g=40$ V. In spite of the rounded transition there is an intermediate regime revealing the characteristic BKT behavior [Eq. (7)], allowing us to estimate R_0, b_R, and T_c. As can be seen in the inset of Fig. 1, depicting $R(T)\exp(b_R|T-T_c|^{-1/2})/R_0$ vs $(1/R_0)\exp(b_R|T-T_c|^{-1/2})$, the rounding of the transition is remarkably consistent with a standard finite-size effect. The horizontal line corresponds to $\xi<L$ where critical behavior can be observed as long as $g(x) \simeq 1$, while the dashed one characterizes the rounded regime where $\xi>L$. Here the scaling function approaches $g(x) \propto x$ and $R(T,L)$ tends to $g \propto L^{-2}$. Independent evidence for BKT behavior was also established in earlier work in terms of the current-voltage characteristics.[2]

Applying this approach to the $R(T)$ data for each gate voltage V_g we obtain good approximations for the values of $T_c(V_g)$, $b_R(V_g)$, and $R_0(V_g)$, in the absence of a finite-size effect. The resulting BKT-transition line is depicted in Fig. 2, displayed as T_c vs $R_\square(T^*)$, the normal-state resistance at $T^*=0.4$ K. We observe that it ends around $R_{\square c}(T^*)$

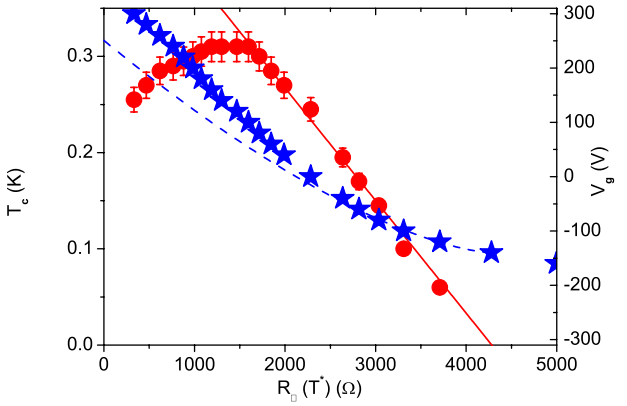

FIG. 2. (Color online) T_c vs $R_\square(T^*)$ (●) and V_g vs $R_\square(T^*)$ (★) at $T^*=0.4$ K. The error bars indicate the uncertainty in the finite-size estimates of T_c. The solid line is $T_c=1.17\times10^{-4}\Delta R(T^*)$ and the dashed one $V_g=V_{gc}+1.39\times10^{-3}\Delta R^{3/2}(T^*)$ with $\Delta R(T^*)=[R_{\square c}(T^*)-R_\square(T^*)]$, $R_{\square c}(T^*)=4.28$ kΩ and $V_{gc}=-140$ V.

$\simeq 4.28$ kΩ where the system is expected to undergo a 2D-QP-transition because T_c vanishes. With reduced $R_\square$ the transition temperature increases and reaches its maximum value, $T_{cm}\simeq 0.31$ K, around $R_\square(T^*)\simeq 1.35$ kΩ. With further reduced resistance T_c decreases. We also included the gate voltage dependence of the normal-state resistance since corrections to Drude behavior ($\sigma\propto n$) have been discussed in the literature for systems exhibiting weak localization as will be demonstrated below.[30,31]

According to the scaling theory of quantum critical phenomena one expects that close to the 2D-QP-transition T_c scales as[12,32]

$$T_c \propto \delta^{z\bar{\nu}}, \tag{10}$$

where δ is the appropriate scaling argument, measuring the relative distance from criticality. $\bar{\nu}$ denotes the critical exponent of the zero-temperature correlation length $\xi(T=0)\propto\delta^{-\bar{\nu}}$ and z the dynamic critical exponent. From Fig. 2 it is seen that the experimental data points to the relationship,

$$T_c \propto \Delta R_\square(T^*) \propto \Delta V_g^{2/3}, \tag{11}$$

close to quantum criticality, where $\Delta R_\square(T^*)=R_{\square c}(T^*)-R_\square(T^*)$. In this context it is important to emphasize that $T_c\propto\Delta R_\square(T^*)$ turns out to be nearly independent of the choice of T^* around $T^*\approx 0.4$ K. So the normal-state sheet resistance $R_\square(T^*)$ is an appropriate scaling variable in terms of $\Delta R_\square(T^*)$. In this case $z\bar{\nu}=1$, while if $\delta=\Delta V_g$, $z\bar{\nu}=2/3$. Since the measured modulation of the gate voltage induced charge density Δn_{2D} scales in the regime of interest as[10]

$$\Delta V_g \propto \Delta n_{2D} \propto T_c^{3/2}, \tag{12}$$

so $z\bar{\nu}=2/3$ if ΔV_g or Δn_{2D} are taken as scaling argument δ. On the other hand it is known that $\delta\propto\Delta n_{2D}$ holds if $(2+z)\bar{\nu}\geq 2$.[33] To check this inequality, given $z\bar{\nu}$, we need an estimate of z. For this purpose we invoke the relation $R_0-R_{0c}\propto\xi_0^{-2}$ [Eq. (6)] and note that the critical amplitude of the finite-temperature correlation length ξ_0 and its zero-temperature counterpart should scale as $\xi_0\propto\xi(T=0)\propto\delta^{-\bar{\nu}}$, so that the scaling relation,

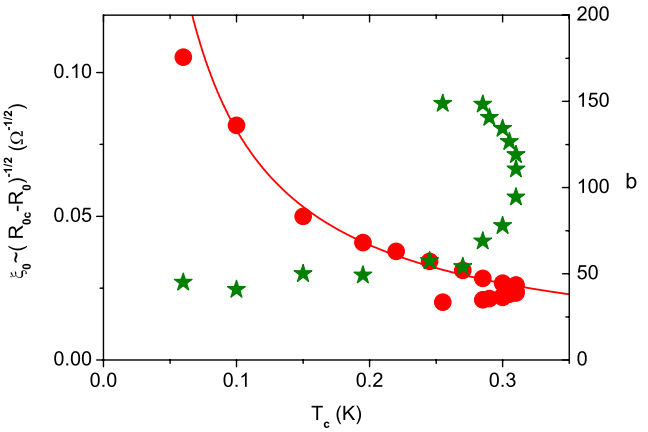

FIG. 3. (Color online) Vortex radius $\xi_0\propto(R_{0c}-R_0)^{-1/2}$ (●) and b (★) vs T_c where $R=3/5R_\square$. The solid line is $\xi_0\propto(R_{0c}-R_0)^{-1/2}=8\times10^{-3}/T_c$ with $R_{0c}=2.7$ kΩ.

$$R_0-R_{0c}\propto\xi_0^{-2}\propto\xi^{-2}(T=0)\propto\delta^{2\bar{\nu}}\propto T_c^{2/z}, \tag{13}$$

holds. Figure 3 depicts the T_c dependence of the vortex core radius $\xi_0\propto\xi(T=0)\propto(R_{0c}-R_0)^{-1/2}$ and b, which is related to the vortex energy E_c. Approaching the 2D-QP-transition we observe that the data point to $\xi(T=0)\propto 1/T_c$, yielding for z the estimate $z\simeq 1$ so that $\bar{\nu}\simeq 2/3$ with $z\bar{\nu}\simeq 2/3$. As these exponents satisfy the inequality $(2+z)\bar{\nu}\geq 2$ (Ref. 33) we identified the correct scaling argument, $\delta\propto\Delta n_{2D}\propto\Delta V_g$. The 2D-QP transition is then characterized by the scaling relations,

$$T_c \propto \delta^{z\bar{\nu}} \propto \Delta R_\square(T^*) \propto \Delta V_g^{2/3} \propto \Delta n_{2D}^{2/3} \propto \xi_0^{-1}, \tag{14}$$

where $\Delta R_\square(T^*)\propto\Delta n_{2D}^{2/3}$ reveals non-Drude behavior in the normal state. The product $z\bar{\nu}\simeq 2/3$ agrees with that found in the electric-field effect tuned 2D-QP-transition in amorphous ultrathin bismuth films[16] and the magnetic-field-induced 2D-QP transition in $Nb_{0.15}Si_{0.85}$ films.[17] On the contrary it differs from the value $z\bar{\nu}\simeq 1$ that has been found in thin $NdBa_2Cu_3O_7$ films using the electric-field-effect modulation of the transition temperature.[19] In any case our estimates, $z\simeq 1$ and $\bar{\nu}\simeq 2/3$ point to a 2D-QP transition which belongs to the 3D-xy universality class.[12]

Figure 3 also depicts the T_c dependence of b, which is related to the vortex energy. Since b tends to a constant in the limit $T_c\to 0$, Eq. (2) implies $db/dT_c=0$ and therewith

$$E_c(T_c) \propto k_B T_c, \tag{15}$$

while the core radius diverges as

$$\xi_0 \propto 1/T_c, \tag{16}$$

in analogy to the behavior of superfluid ^{4}He films where T_c was tuned by varying the film thickness.[34] A linear relationship between the vortex core energy and T_c was also predicted for heavily underdoped cuprate superconductors.[35] Furthermore, an increase in the vortex core radius with reduced T_c was also observed in underdoped $YBa_2Cu_3O_y$ (Ref. 36) and $La_{2-x}Sr_xCuO_4$.[37] The 2D-QP transition is then also characterized by vortices having an infinite radius and vanishing core energy. As T_c increases from the 2D-QP transi-

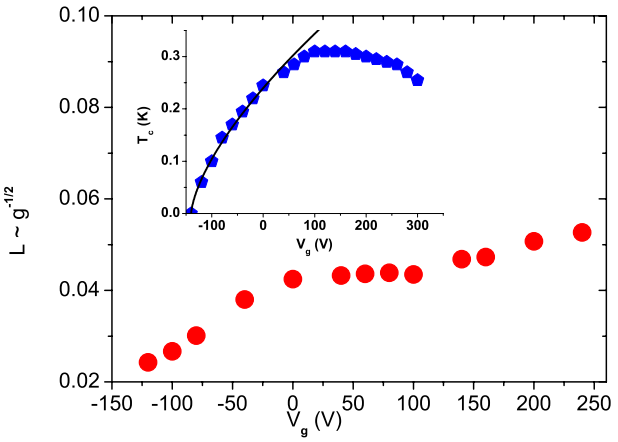

FIG. 4. (Color online) Gate voltage dependence of the limiting length L in terms of $L \propto g^{-1/2}$ *vs.* V_g. The inset shows T_c vs V_g. The solid line is $T_c = 8.9 \times 10^{-3}(V_g - V_{gc})^{2/3}$(K) indicating the leading quantum critical behavior [Eq. (14)] with $z\bar{\nu} \simeq 2/3$.

tion, the core radius shrinks, while the vortex energy increases. We also observe that the rise of T_c is limited by a critical value of the core radius and that the maximum $T_c(T_{cm} \simeq 0.31$ K) is distinguished by an infinite slope of both, the vortex radius and b. Finally, after passing T_{cm} the vortex core radius ξ_0 continues to decrease with reduced T_c while b increases further.

Next we explore the gate voltage dependence of the limiting length. Indeed, its presence or absence allows us to discriminate between an intrinsic or extrinsic limiting length. For this purpose we performed the finite scaling analysis outlined in Fig. 1 for various gate voltages. In the finite-size dominated regime, $\xi > L$, the finite-size scaling form [Eq. (8)] reduces to $R(T)\exp(b_R|T-T_c|^{-1/2})/R_0 = g(x) \propto (g/R_0)\exp(b_R|T-T_c|^{-1/2})$ with $g \propto 1/L^2$, so g probes, if there is any, the gate voltage dependence of L. In Fig. 4 we summarized the resulting gate voltage dependence of $L \propto g^{-1/2}$. It is seen that the limiting length is nearly gate voltage independent down to $V_g = 0$ V. This points to the presence of inhomogeneities preventing the correlation length to grow beyond the lateral extent of the homogeneous domains. On the contrary, for negative gate voltages L decreases by approaching the QP transition as T_c does. The resulting broadening of the BKT-transition with reduced V_g and T_c is apparent in the temperature dependence of the sheet resistance.[10] A potential candidate for a gate voltage dependent limiting length is the failure of cooling at very low temperatures.[18] In this case the correlation length cannot grow beyond its value at the temperature T_f where the failure of cooling sets in. Invoking Eq. (1) in the limit $T_c \to 0$ we obtain $L_f = \xi_0 \exp(2\pi/(bT_f^{1/2}) \propto 1/T_c$, because $\xi_0 \propto 1/T_c$ and b remains finite in the limit $T_c \to 0$ (see Fig. 3). Contrariwise we observe in Fig. 4 that L decreases with T_c. According to this electrostatic tuning does not change the carrier density only but the inhomogeneity landscape as well.

In any case, the agreement with BKT behavior, limited by a standard finite-size effect, allows us to discriminate the rounded transition from other scenarios, including strong disorder which destroys the BKT behavior. It also provides the basis to estimate T_c, b_R, and R_0, and with that b and $\xi_0 \propto R_0^{-1/2}$ with reasonable accuracy. The resulting BKT-transition line ends at $V_{gc} \simeq -140$ V, where T_c vanishes and the system undergoes a 2D-QP transition. After passing this transition T_c increases with reduced negative gate voltage, reaches its maximum, $T_{cm} \simeq 0.31$ K, around $V_g \simeq 110$ V and decreases with further increase in the positive gate voltage. Remarkably enough, this uncovers a close analogy to the doping dependence of T_c in a variety of bulk cuprate superconductors,[12,38] where after passing the so-called underdoped limit T_c reaches its maximum with increasing dopant concentration. With further increase in the dopant concentration T_c decreases and finally vanishes in the overdoped limit. This phase-transition line is thought to be a generic property of bulk cuprate superconductors. There is, however, an essential difference. Cuprates are bulk superconductors and the approach to the underdoped limit, where the QP transition occurs, is associated with a 3D to 2D crossover,[12,38] while in the present case the system is and remains 2D, as the consistency with BKT critical behavior reveals. Furthermore, a superconducting dome (in the T versus doping phase diagram) was also observed in bulk doped $SrTiO_3$ that is close to the system under study.[39,40]

B. INSULATING PHASE

Supposing that the insulating phase is a weakly localized Fermi liquid the sheet conductivity should scale as[41]

$$\sigma_\square(T) = \sigma_{\square 0} + d\,\ln(T), \tag{17}$$

where $d = e^2/(\pi h) \simeq 1.23 \times 10^{-5}\ \Omega^{-1}$ is generically attributed to electron-electron interaction,[42] while $\sigma_{\square 0}$ is expected to depend on the gate voltage. In Fig. 5(a) we depicted $\sigma_\square - \sigma_{\square 0}$ vs T for various gate voltages V_g by adjusting $\sigma_{\square 0}$ to achieve a data collapse at sufficiently high temperatures. The resulting gate voltage dependence of $\sigma_{\square 0}$, consistent with

$$\sigma_{\square 0}(V_g) = \sigma_{\square s} - 5.9 \times 10^{-6}|V_g - V_{gc}|^{2/3}(\Omega^{-1}),$$

$$\sigma_{\square s} = 2.52 \times 10^{-4}(\Omega^{-1}), \tag{18}$$

is shown in Fig. 5(b). An important feature of the data is the consistency with a weakly localized Fermi liquid because the coefficient d is close to $d = e^2/(\pi h)$. In any case, more extended evidence for weak localization emerges from the magnetoconductivity presented below (Fig. 9).

A very distinct temperature dependence of the conductivity occurs at quantum criticality, $V_g = -140$ V $\simeq V_{gc}$. Indeed, the dashed line in Fig. 5(a) and the solid one in Fig. 6 indicate that in the limit $T \to 0$ the system tends toward a critical value. According to the plots shown in Fig. 6 the limiting behavior is well described by

$$\sigma_\square(T, V_{gc}) = \sigma_{\square s}(V_{gc}) - 9.782 \times 10^{-4}\ \mathrm{T}^2. \tag{19}$$

Note that our estimate $\sigma_\square(T=0, V_{gc}) = \sigma_{\square 0}(V_{gc}) = \sigma_{\square s} = 2.52 \times 10^{-4}\ \Omega^{-1}$ is comparable to the quantum unit of conductivity $4e^2/h \simeq 1.55 \times 10^{-4}\ \Omega^{-1}$ for electron pairs, emphasizing the importance of quantum effects. The T^2 dependence points to Fermi-liquid behavior in the regime $k_B T \ll \hbar\omega_D, E_F$ where electron-electron scattering dominates. ω_D is the Debye fre-

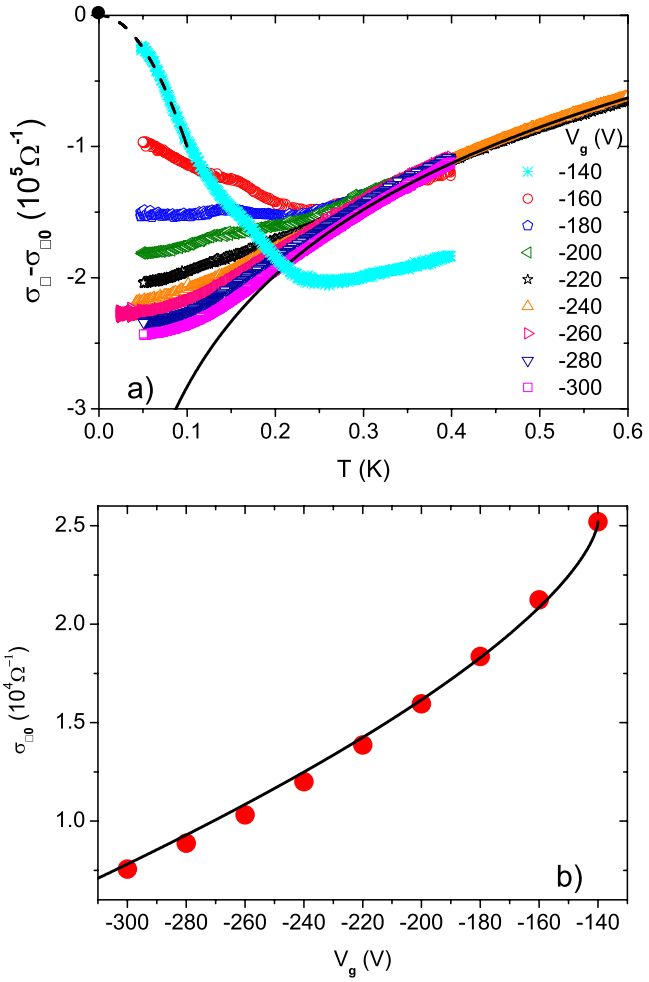

FIG. 5. (Color online) (a) $\sigma_\square - \sigma_{\square 0}$ vs T for various gate voltages V_g. The solid line is $\sigma_\square - \sigma_{\square 0} = d\ln(T)(\Omega^{-1})$ with $d \simeq 1.23 \times 10^{-5}\ \Omega^{-1}$ and $\sigma_{\square 0}(V_g)$ taken from Fig. 5(b). The dot at the origin marks the quantum critical point and the dashed line is Eq. (19) indicating the low-temperature behavior of the sheet conductivity at the quantum critical point. (b) $\sigma_{\square 0}$ vs V_g. The solid line is Eq. (18) with $V_{gc} = -140$ V.

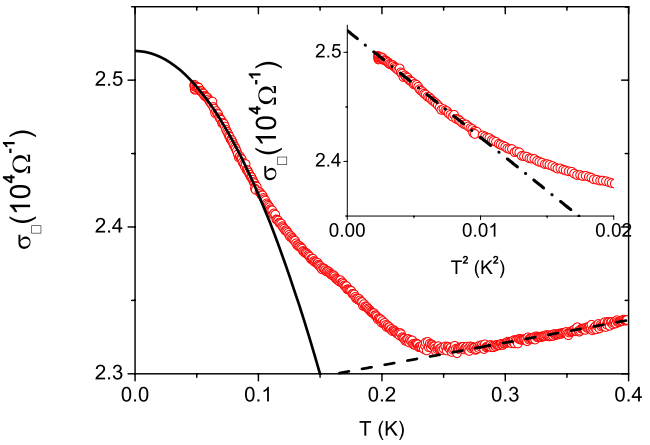

FIG. 6. (Color online) $\sigma_\square(V_{gc}, T)$ vs T and in the inset vs T^2 at $V_{gc} = -140$ V. The solid line, indicating consistency with T^2 is Eq. (19), while the dashed line is $\sigma_\square(V_{gc}, T) = 2.275 \times 10^{-4} + 1.54 \times 10^{-5}\ \mathrm{T}(\Omega^{-1})$. The dash-dot one in the inset is again Eq. (19).

quency and E_F denotes the Fermi energy. At higher temperature we observe a crossover to a linear T-dependent conductivity marked by the dash-dot line. Recent theories on the conductivity of 2D Fermi liquids predict such a linear T dependence.[43] From Eqs. (17) and (18), describing the data in the weakly localized regime rather well, it also follows that the normal-state conductivity at $T^* = 0.4$ K scales as $\sigma_{\square c}(T^*) - \sigma_\square(T^*) \propto 10^{-6}|V_g - V_{gc}|^{2/3}$. Together with the empirical scaling relation [Eq. (14)], $|V_g - V_{gc}| \propto \Delta n_{2D}$, it points to non-Drude behavior in the normal state.

Considering the temperature dependence of the sheet conductivity below quantum criticality ($V_g = -140\ \mathrm{V} \simeq V_{gc}$), Fig. 5(a) reveals at sufficiently high-temperature remarkable agreement with the $\ln(T)$ behavior, characteristic for weak localization. On the contrary, in the low-temperature regime and even rather deep in the insulating phase ($V_g = -300$ V), systematic deviations occur in terms of saturation and an upturn as quantum criticality is approached ($V_{gc} = -140$ V). Because the conductivity of a weakly localized insulator is not expected to saturate in the zero-temperature limit[44,45] this behavior appears to be a finite-size effect, preventing the diverging length associated with localization,[41] $\xi_{\mathrm{loc}} \propto d|\ln(T)|$, to grow beyond L, the limiting length already identified in the context of the rounded BKT transition (Fig. 4). In the present case finite-size scaling predicts that $\sigma_\square(T)$ should scale as

$$\frac{\sigma_\square(T) - \sigma_{\square c}}{d\ln(T)} = g(y), \quad y = L/\xi_{\mathrm{loc}} \propto L/[d|\ln(T)|]. \tag{20}$$

$g(y)$ is the finite-size scaling function which tends to 1 for $y < 1$. In this case the approach to the insulating ground state can be seen, while for $y > 1$ the crossover to $g(y) \to y$ sets in and $\sigma_\square(T)$ approaches the finite-size dominated regime, where

$$\frac{\sigma_\square(T) - \sigma_{\square c}}{d\ln(T)} = g_L/[d|\ln(T)|], \quad g_L \propto L. \tag{21}$$

A glance at Fig. 7, depicting $[\sigma_\square(T) - \sigma_{\square 0}]/[d\ln(T)]$ vs $1/[d\ln(T)]$ at $V_g = -220$, -240 and -300 V, reveals that the systematic deviations from the characteristic weak localization temperature dependence are fully consistent with a standard finite-size effect. Accordingly, the saturation and upturns seen in Fig. 5 at low temperatures are attributable to a finite-size effect, while in a homogeneous and infinite system the data should collapse on the solid line in Fig. 5(a). An essential exception is $V_g = -140$ V. Here the interface approaches the metallic quantum critical point (see Fig. 5), metallic because the sheet conductivity remains finite, approaching $\sigma_\square(T = 0, V_{gc}) = \sigma_{\square 0}(V_{gc}) = \sigma_{\square s} \simeq 2.52 \times 10^{-4}\ \Omega^{-1}$ [Eq. (19)] in the limit $T \to 0$.

Figure 7 also reveals that the limiting length, $L \propto g_L$, depends in the insulating phase on the gate voltage as well. The resulting dependence, $L(V_g) \propto g_L(V_g)$, is shown in Fig. 8. In analogy to the limiting length associated with the BKT-transition (Fig. 4) it decreases by approaching quantum criticality at $V_g \simeq -140$ V. As a reduction in L enhances deviations from the asymptotic behavior this feature accounts for

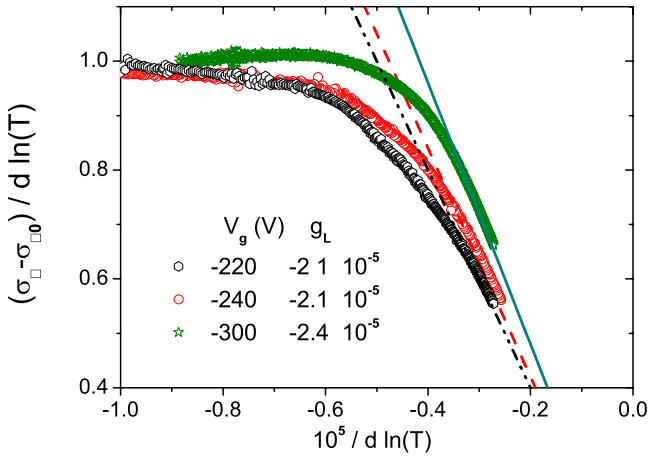

FIG. 7. (Color online) $[\sigma_{\square}(T)-\sigma_{\square 0}]/[d\ \ln(T)]$ vs $1/[d|\ln(T)|]$ at $V_g=-220$, -240 and -300 V with $d=1.23\times10^{-5}$ Ω^{-1}. The lines correspond to Eq. (21) providing a measure for L in terms of $|g_L| \propto L$.

the saturation and upturns seen in Fig. 5(a). Supposing that the limiting length is set by the failure of cooling below the temperature T_f then L is set by $L_f=\xi_{\mathrm{loc}}(T_f)\propto d|\ln(T_f)|$ and with that independent of the gate voltage, in disagreement with Fig. 8. Accordingly, in analogy to the BKT transition, the limiting length appears to be attributable to a electrostatic mediated change in the inhomogeneity landscape.

Direct experimental evidence for a limiting length emerges from the work of Ilani *et al.*[46] A single electron transistor was used as a local electrostatic probe to study the underlying spatial structure of the metal-insulator transition in two dimensions. The measurements show that as the transition is approached from the metallic side, a new phase emerges that consists of weakly coupled fragments of the two-dimensional system. These fragments consist of localized charge that coexists with the surrounding metallic phase. As the density is lowered into the insulating phase, the number of fragments increases on account of the disappearing metallic phase. The measurements suggest that the metal-insulator transition is a result of the microscopic restructuring that occurs in the system. On the other hand, we have

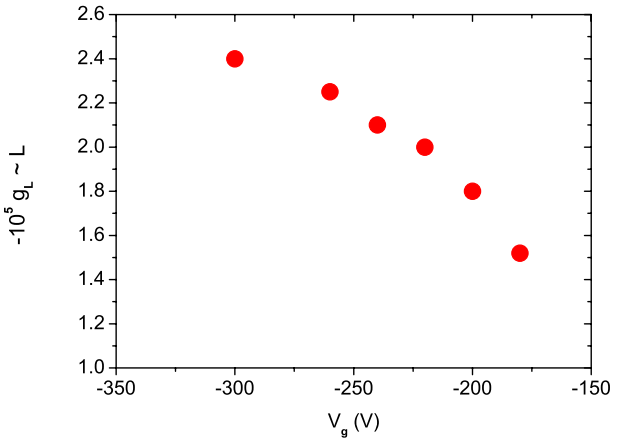

FIG. 8. (Color online) $-g_L\propto L$ vs V_g derived from finite-size scaling plots as shown in Fig. 7 with Eq. (21).

seen that the limiting length associated with the resulting inhomogeneities depends on the gate voltage (see Figs. 4 and 8).

Further evidence for a weakly localized insulating phase stems from the observed negative magnetoresistance.[10] An applied magnetic field leads to a new length given by the size of the first Landau orbit, or magnetic length, $L_H=[\Phi_0/(2\pi H)]^{1/2}$, which decreases with growing field strength. Once its size becomes comparable to the dephasing length L_{Th} (distance between inelastic collisions)[47] weak localization is suppressed. In $D=2$ the following formula for the magnetoconductivity was obtained:[48,49]

$$\sigma_{\square}=\sigma_{\square 0}+c[\psi(1/2+1/x)+\ln(x)],\quad c=\frac{\alpha^* e^2}{\pi h}, \tag{22}$$

where ψ denotes the digamma function, α^* is a constant of the order of unity,[49] and

$$x=\frac{8\pi L_{Th}^2 H}{\Phi_0}. \tag{23}$$

In the limit $x\gg 1$ it reduces to

$$\sigma_{\square}=\sigma_{\square 0}+\frac{\alpha^* e^2}{\pi h}[-1.96+\ln(x)], \tag{24}$$

while in the limit $x\to 0$

$$\sigma_{\square}-\sigma_{\square 0}\propto H^2, \tag{25}$$

holds. Here

$$\frac{d\sigma_{\square}}{d\ \ln(H)}=\frac{\alpha^* e^2}{\pi h}\simeq \alpha^* 1.24\times 10^{-5}\ \ \Omega^{-1} \tag{26}$$

applies. In Fig. 9 we compare the experimental data with the theoretical predictions. The data agree reasonably well with the characteristic weak localization behavior [Eq. (22)], while the asymptotic $\ln(H)$ behavior [Eq. (24)] is not fully attained. The resulting estimates for $d\sigma_{\square}/d\ \ln(H)$ are close to $e^2/(\pi h)\simeq 1.24\times 10^{-5}$ Ω^{-1} and consistent with the zero field temperature dependence of the sheet conductivity, $\sigma_{\square}(T)=\sigma_{\square 0}+d\ \ln(T)$, with $d=e^2/(\pi h)$ [see Fig. 5(a)]. An analogous treatment of the magnetoresistance data of a nonsuperconducting sample of Brinkman *et al.*[5] yields $8\pi L_{Th}^2/\Phi_0=2.862$ T^{-1} and $c=\alpha^* e^2/\pi h=4.8\times 10^{-5}$ Ω^{-1}, so c adopts in "superconducting" and "nonsuperconducting" samples substantially different values. In any case, our analysis of the magnetoconductivity uncovers a weakly localized insulating phase, consistent with the $\ln(T)$ temperature dependence of the zero field counterpart at sufficiently high temperatures, and non-Drude behavior in the normal state.

C. Quantum phase transition

Traditionally the interpretation of experimental data taken close to the 2D-QP-transition was based on the quantum scaling relation,[14,15,50]

$$R_{\square}(T,\delta)=R_{\square s}G(x),\quad x=c\,\delta/T^{1/z\bar{\nu}}. \tag{27}$$

$G(x)$ is a scaling function of its argument and $G(0)=1$, so at quantum criticality the system is metallic with sheet resis-

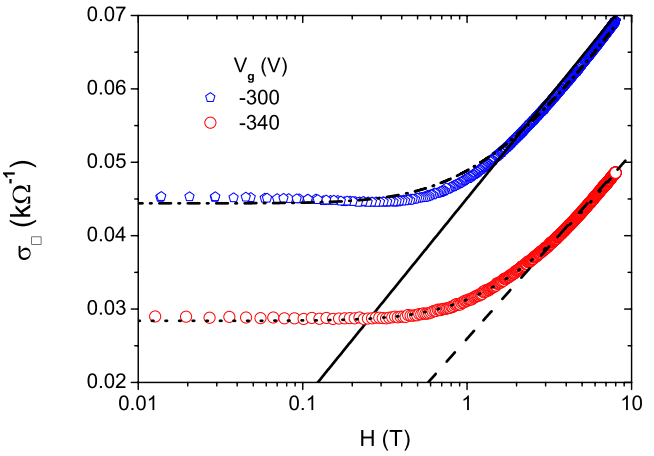

FIG. 9. (Color online) Magnetoconductivity $\sigma_{\square}$ vs H, applied perpendicular to the interface, at $T=0.03$ K and $V_g=-300$ V and -340 V. The solid line is $\sigma_{\square}=4.51\times10^{-2}+1.2\times10^{-2}$ ln(H)kΩ^{-1}, the dashed one $\sigma_{\square}=2.6\times10^{-2}+1.1\times10^{-2}$ ln(H)kΩ^{-1}, the dotted and dash-dot curves are Eq. (22) with the $\sigma_{\square 0}$, $8\pi L_{TH}^2/\Phi_0$ and $c=\alpha^* e^2/(\pi h)$ values 0.0284 kΩ^{-1}, 2.906 T^{-1}, 1.46×10^{-5} Ω^{-1} for $V_g=-340$ V and 0.044 kΩ^{-1}, 4.068 T^{-1}, 1.46×10^{-5} Ω^{-1}, at $V_g=-300$ V. Note that $8\pi L_{TH}^2/\Phi_0=2.906$ T^{-1} corresponds to $L_{TH}\simeq1.55\times10^{-6}$ cm whereupon $L_H=L_{TH}$ at $H=1.37$ T.

tance $R_{\square s}$. The BKT line is then fixed by $x_c=c\,\delta/T_c^{1/z\bar{\nu}}$, whereby T_c vanishes as $T_c\propto\delta^{z\bar{\nu}}\propto\xi^{-z}(T=0)$ [Eq. (14)]. c is a nonuniversal parameter and δ the appropriate scaling argument, measuring the relative distance from criticality. This scaling form follows by noting that the divergence of $\xi(T=0)\propto\delta^{-\bar{\nu}}$ is at finite-temperature cutoff by a length L_T, which is determined by the temperature: $L_T\propto T^{-1/z}$. Thus $G(x)$ is a finite-size scaling function because $x\propto[L_T/\xi(T=0)]^{1/\bar{\nu}}\propto\delta/T^{1/z\bar{\nu}}$. The data for $R_{\square}(T,\delta)$ plotted vs $\delta/T^{1/z\bar{\nu}}$ should then collapse onto two branches joining at $R_{\square s}$. The lower branch stems from the superconducting and the upper one from the insulating phase. To explore the consistency with the critical BKT behavior we note that in the limit $T_c\to0$ the relation,

$$\frac{R_{KT}(T,V_g)}{R_0(V_g)}=\exp\left(-\frac{b_R(V_g)}{[T-T_c(V_g)]^{1/2}}\right)=G\left(\frac{V_g-V_{gc}}{T^{1/z\bar{\nu}}}\right), \tag{28}$$

should apply. Indeed, the BKT-scaling form of the resistance applies for any $T\gtrsim T_c$ because the universal critical behavior close to T_c is entirely classical.[51] On the contrary T_c, b_R, and the critical amplitude R_0 are nonuniversal quantities which depend on the tuning parameter. Furthermore, they are renormalized by quantum fluctuations. In any case, the data plotted as $R_{KT}(T,V_g)/R_0(V_g)$ vs $(V_g-V_{gc})/T^{1/z\bar{\nu}}$ should collapse on a single curve and approach one close to quantum criticality. In Fig. 10 we depicted this scaling plot, derived from $R_0(V_g)$, $b_R(V_g)$, and $T_c(V_g)$ for $z\bar{\nu}=2/3$. Apparently, the flow to the quantum critical point is well confirmed. Furthermore, noting that close to the QP-transition $b_R(V_g)\propto T_c^{1/2}$, because $b_R=4\pi T_c^{1/2}/b$ [Eq. (3)] and $b\simeq$ const. (see Fig. 3), the vortex core energy scales as $E_c\propto k_B T_c$ [Eq. (15)], the scaling function adopts with $z\bar{\nu}=2/3$ and $T_c\propto(V_g-V_{gc})^{2/3}$ [Eq. (14)] the form

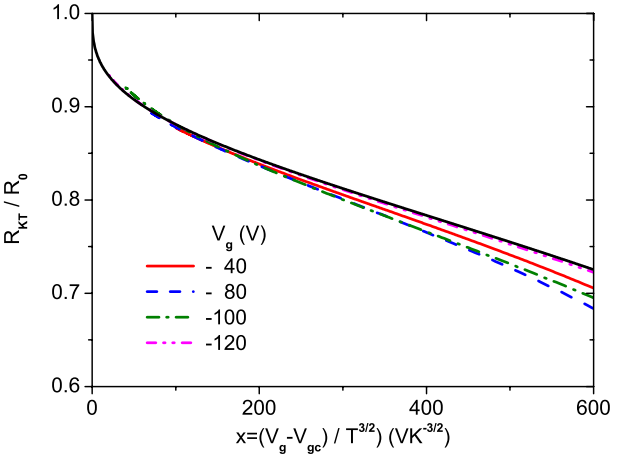

FIG. 10. (Color online) $R_{KT}(V_g,T)/R_0(V_g)$ vs $(V_g-V_{gc})/T^{3/2}$ for various V_g's. The solid line is Eq. (29) with $\tilde{a}=0.0248$ and $\tilde{b}=0.0081$ in K$^{3/2}$ V^{-1}.

$$G(x)\simeq\exp(-\tilde{a}x^{1/3}/(1-\tilde{b}x^{2/3})^{1/2}),\quad x=\frac{V_g-V_{gc}}{T^{3/2}}, \tag{29}$$

shown by the solid line in Fig. 10. Since $V_g-V_{gc}\propto T_c^{1/z\bar{\nu}}\propto T_c^{3/2}$ and $b_R=4\pi T_c^{1/2}/b$ is related to the vortex energy in terms of b [Eq. (3)], the scaling function is controlled by the BKT line and the vortex core energy, while the vortex core radius enters the prefactor via $R_0(V_g)-R_{0c}\propto\xi_0^{-2}\propto\xi^{-2}(T=0)\propto T_c^2$ [Eq. (13)]. Noting that $\tilde{a}=4\pi a^{1/2}/b$ and $\tilde{b}=a$, where a is given in terms of $T_c=a(V_g-V_{gc})^{2/3}$(K) with $a\simeq8.9\times10^{-3}$ (see Fig. 4) and $b\simeq50$ (Fig. 3) we obtain $\tilde{a}\simeq0.0237$ and $\tilde{b}=a\simeq0.0089$, in reasonable agreement with the fit parameters yielding the solid line in Fig. 10. This uncovers the consistency and reliability of our estimates along the BKT line. In this context it should be kept in mind that our analysis of the insulating state is limited by the finite-size effect, preventing to approach the zero-temperature regime.

On the contrary, in the insulating phase we observed that the sheet conductivity scales according to Eqs. (17) and (18) as

$$\frac{\sigma_{\square}(T,V_g)}{\sigma_{\square s}}=1-\frac{5.9\times10^{-6}}{\sigma_{\square s}}|V_g-V_{gc}|^{2/3}+\frac{d}{\sigma_{\square s}}\ln(T). \tag{30}$$

which is incompatible with the standard scaling form [Eq. (27)]. Indeed, it involves two independent lengths. $\xi_{ld}\propto1/|\ln(T)|$, the diverging length associated with localization[41] and $\xi(T=0)\propto|\Delta V_g|^{-2/3}$, the zero-temperature correlation length [Eq. (14)]. In this context it should be kept in mind that our analysis of the insulating state does not extend to zero temperature because Eq. (30) applies at finite temperatures only. As T is reduced further the question of what happens in the insulating phase remains.

To complete the BKT- and 2D-QP-transition scenario measurements of the magnetic penetration depth, $\lambda(T)$, would be required. At the BKT-transition T_c and $\lambda(T)$ are related by

$$\rho_s(T_c) = \frac{d\Phi_0^2}{16\pi^3\lambda^2(T_c)} = \frac{2}{\pi}k_B T_c, \tag{31}$$

while $\rho_s(T)=0$ above T_c. ρ_s is the 2D superfluid density and d is the thickness of the superconducting sheet.[52] The presence or absence of the resulting Nelson-Kosterlitz jump would then allow to discriminate experimentally between weak and strong disorder. In this context we note that there is the Harris criterion,[53] which states that short-range correlated and uncorrelated disorder is irrelevant at the unperturbed critical point, provided that $2-D\nu<0$, where D is the dimensionality of the system and ν the critical exponent of the finite-temperature correlation length. With $D=2$ and $\nu=\infty$, appropriate for the BKT transition,[21] any rounding of the jump should then be attributable to the finite-size effect stemming from the limiting length L. Furthermore, there is the quantum counterpart of the Nelson-Kosterlitz relation, stating that

$$\frac{d}{\lambda^2(T=0)} = \frac{16\pi^3 k_B T_c Q_2}{\Phi_0^2}, \tag{32}$$

close to the 2D-QP transition.[12,13,32] Q_2 is a dimensionless critical amplitude bounded by[54]

$$\frac{2}{\pi} < Q_2 < 1.11. \tag{33}$$

The lower bound corresponds to the BKT line, $d/\lambda^2(T=0) \simeq 1.03T_c$ with d, λ in *cm* and T_c in K. Below this line the superfluid order would become unstable to unbinding of vortices. The upper bound, corresponds to $d/\lambda^2(T=0) \simeq 1.61T_c$ and the transition at $T=0$ belongs to the BKT-universality class and consequently at T_c the superfluid density exhibits the universal discontinuity. Given our evidence for a $(2+1)$-*xy* QP transition, quantum fluctuations are present and expected to reduce Q_2 from its maximum value, while the finite-temperature transition remains again in the BKT-universality class.[54] Correspondingly, measurements of the temperature and gate voltage dependence of the superfluid density would be desirable to explore the observed BKT behavior, weak localization and Fermi liquid features further.

III. SUMMARY AND DISCUSSION

In summary, we have shown that the electrostatically tuned phase-transition line at the $LaAlO_3/SrTiO_3$ interface, observed by Caviglia *et al.*,[10] is consistent with a BKT-line ending at a 2D-quantum critical point with critical exponents $z \simeq 1$ and $\bar{\nu} \simeq 2/3$, so the universality class of the transition appears to be that of the classical 3D-*xy* model. We have shown that the rounding of the BKT-transition line and the saturation of the sheet conductivity close to the QP transition are remarkably consistent with a gate voltage dependent finite-size effect. According to this, electrostatic tuning does not change the carrier density only but the inhomogeneity landscape as well. Taking the resulting finite-size effect into account we provided consistent evidence for a weakly localized insulator separated from the superconducting phase by a metallic ground state at quantum criticality. Consistent with the non-Drude behavior in the normal state, characteristics of weak localization have been identified in both, the temperature and magnetic-field dependence of the conductivity. The conductivity along the BKT-transition line was found to agree with the standard scaling form of quantum critical phenomena, while in the weakly localized insulating phase it appears to fail in the accessible temperature regime. As in the quantum scaling approach the scaling function is unknown we obtained its form in the superconducting phase. It is controlled by the BKT-phase transition line and the vortex energy. In addition we explored the T_c dependence of the vortex core radius and the vortex energy. As the nature of the metallic ground state at quantum criticality is concerned, the limiting T^2 dependence of the sheet conductivity points to Fermi-liquid behavior, consistent with the evidence for weak localization in the insulating phase and non-Drude behavior in the normal state. In conclusion we have shown that the appearance of metallicity at the interface between insulators, a wonderful example of how subtle changes in the structure of these systems can lead to fundamental changes in physical properties, is a source of rich physics in two dimensions.

ACKNOWLEDGMENTS

This work was partially supported by the Swiss National Science Foundation through the National Center of Competence in Research, and "Materials with Novel Electronic Properties, MaNEP" and Division II.

*tschnei@physik.unizh.ch

[1] A. Ohtomo and H. Y. Hwang, Nature (London) **427**, 423 (2004).
[2] N. Reyren, S. Thiel, A. D. Caviglia, L. Fitting Kourkoutis, G. Hammerl, C. Richter, C. W. Schneider, T. Kopp, A.-S. Rüetschi, D. Jaccard, M. Gabay, D. A. Muller, J.-M. Triscone, and J. Mannhart, Science **317**, 1196 (2007).
[3] E. Bousquet, M. Dawber, N. Stucki, C. Lichtensteiger, P. Hermet, S. Gariglio, J.-M. Triscone, and P. Ghosez, Nature (London) **452**, 732 (2008).
[4] S. Okamoto and A. J. Millis, Nature (London) **428**, 630 (2004).
[5] A. Brinkman, M. Huijben, M. Van Zalk, J. Huijben, U. Zeitler, J. C. Maan, W. G. Van der Wiel, G. Rijnders, D. H. A. Blank, and H. Hilgenkamp, Nature Mater. **6**, 493 (2007).
[6] P. R. Willmott, S. A. Pauli, R. Herger, C. M. Schlepütz, D. Martoccia, B. D. Patterson, B. Delley, R. Clarke, D. Kumah, C. Cionca, and Y. Yacoby, Phys. Rev. Lett. **99**, 155502 (2007).
[7] W. Siemons, G. Koster, H. Yamamoto, W. A. Harrison, G. Lucovsky, Th. H. Geballe, D. H. A. Blank, and M. R. Beasley,

Phys. Rev. Lett. **98**, 196802 (2007).
[8] G. Herranz, M. Basletic, M. Bibes, C. Carretero, E. Tafra, E. Jacquet, K. Bouzehouane, C. Deranolt, A. Hamzic, J. M. Broto, A. Barthelemy, and A. Fert, Phys. Rev. Lett. **98**, 216803 (2007).
[9] S. A. Pauli and P. R. Willmott, J. Phys.: Condens. Matter **20**, 264012 (2008).
[10] A. D. Caviglia, S. Gariglio, N. Reyren, D. Jaccard, T. Schneider, M. Gabay, S. Thiel, G. Hammerl, J. Mannhart, and J.-M. Triscone, Nature (London) **456**, 624 (2008).
[11] S. L. Sondhi, S. M. Girvin, J. P. Carini, and D. Shahar, Rev. Mod. Phys. **69**, 315 (1997).
[12] T. Schneider and J. M. Singer, *Phase Transition Approach to High Temperature Superconductivity* (Imperial College Press, London, 2000).
[13] T. Schneider, in *The Physics of Superconductors*, edited by K. Bennemann and J. B. Ketterson (Springer, Berlin, 2004), p. 111.
[14] N. Marković, C. Christiansen, A. Mack, and A. M. Goldman, Phys. Status Solidi B **218**, 221 (2000).
[15] A. M. Goldman, Physica E **18**, 1 (2003).
[16] K. A. Parendo, K. H. Sarwa B. Tan, A. Bhattacharya, M. Eblen-Zayas, N. E. Staley, and A. M. Goldman, Phys. Rev. Lett. **94**, 197004 (2005).
[17] H. Aubin, C. A. Marrache-Kikuchi, A. Pourret, K. Behnia, L. Bergé, L. Dumoulin, and J. Lesueur, Phys. Rev. B **73**, 094521 (2006).
[18] K. A. Parendo, K. H. Sarwa B. Tan, and A. M. Goldman, Phys. Rev. B **73**, 174527 (2006).
[19] D. Matthey, N. Reyren, J.-M. Triscone, and T. Schneider, Phys. Rev. Lett. **98**, 057002 (2007).
[20] V. L. Berezinskii, Sov. Phys. JETP **32**, 493 (1971).
[21] J. M. Kosterlitz and D. J. Thouless, J. Phys. C **6**, 1181 (1973).
[22] M. E. Fisher and M. N. Barber, Phys. Rev. Lett. **28**, 1516 (1972).
[23] V. Privman and M. E. Fisher, Phys. Rev. B **30**, 322 (1984).
[24] V. Ambegaokar, B. I. Halperin, D. R. Nelson, and E. D. Siggia, Phys. Rev. B **21**, 1806 (1980).
[25] D. Finotello and F. M. Gasparini, Phys. Rev. Lett. **55**, 2156 (1985).
[26] Lindsay M. Steele, Ch. J. Yeager, and D. Finotello, Phys. Rev. Lett. **71**, 3673 (1993).
[27] D. R. Tilley and J. Tilley, *Superfluidity and Superconductivity* (Adam Hilger, Bristol, 1990).
[28] A. J. Dahm, Phys. Rev. B **29**, 484 (1984).
[29] S. W. Pierson, M. Friesen, S. M. Ammirata, J. C. Hunnicutt, and LeRoy A. Gorham, Phys. Rev. B **60**, 1309 (1999).
[30] B. L. Altshuler, A. G. Aronov, and D. E. Khmelnitskii, J. Phys. C **15**, 7367 (1982).
[31] S. Chakravarty and A. Schmid, Phys. Rep. **140**, 193 (1986).
[32] Kihong Kim and Peter B. Weichman, Phys. Rev. B **43**, 13583 (1991).
[33] M. P. A. Fisher, P. B. Weichman, G. Grinstein, and D. S. Fisher, Phys. Rev. B **40**, 546 (1989).
[34] H. Cho and G. A. Williams, Phys. Rev. Lett. **75**, 1562 (1995).
[35] L. Benfatto, C. Castellani, and T. Giamarchi, Phys. Rev. B **77**, 100506(R) (2008).
[36] J. E. Sonier *et al.*, Phys. Rev. B **76**, 134518 (2007).
[37] R. Kadono *et al.*, Phys. Rev. B **69**, 104523 (2004).
[38] T. Schneider, Physica B **326**, 289 (2003).
[39] J. F. Schooley, W. R. Hosler, and M. L. Cohen, Phys. Rev. Lett. **12**, 474 (1964).
[40] J. F. Schooley, W. R. Hosler, E. Ambler, J. H. Becker, M. L. Cohen, and C. S. Koonce, Phys. Rev. Lett. **14**, 305 (1965).
[41] P. A. Lee and T. V. Ramakrishnan, Rev. Mod. Phys. **57**, 287 (1985).
[42] Ya. M. Blanter, V. M. Vinokur, and L. I. Glazman, Phys. Rev. B **73**, 165322 (2006).
[43] G. Zala, B. N. Narozhny, and I. L. Aleiner Phys. Rev. B **64**, 214204 (2001); **65**, 020201(R) (2001).
[44] F. Marquardt, J. von Delft, R. A. Smith, and V. Ambegaokar, Phys. Rev. B **76**, 195331 (2007).
[45] J. von Delft, F. Marquardt, R. A. Smith, and V. Ambegaokar, Phys. Rev. B **76**, 195332 (2007).
[46] S. Ilani, A. Yacoby, D. Mahalu, and H. Shtrikman, Science **292**, 1354 (2001).
[47] D. J. Thouless, Phys. Rev. Lett. **39**, 1167 (1977).
[48] B. L. Altshuler, D. Khmel'nitzkii, A. I. Larkin, and P. A. Lee, Phys. Rev. B **22**, 5142 (1980).
[49] S. Hikami, A. I. Larkin, and Y. Nagaoka, Prog. Theor. Phys. **44**, 1288 (1980).
[50] M. P. A. Fisher, G. Grinstein, and S. M. Girvin, Phys. Rev. Lett. **64**, 587 (1990).
[51] M. Vojta, Rep. Prog. Phys. **66**, 2069 (2003).
[52] D. R. Nelson and J. M. Kosterlitz, Phys. Rev. Lett. **39**, 1201 (1977).
[53] A. B. Harris, J. Phys. C **7**, 1671 (1974).
[54] I. F. Herbut and M. J. Case, Phys. Rev. B **70**, 094516 (2004).